4D Metamaterials with Zero Poisson's Ratio, Shape Recovery, and Energy Absorption Features

*Ramin Hamzehei, Ahmad Serjouei, Nan Wu, Ali Zolfagharian, and Mahdi Bodaghi**

This article introduces novel 3D zero Poisson's ratio (ZPR) metamaterials for reversible energy absorption applications fabricated by 4D printing technology. The designs are introduced based on piecemeal energy absorption (PEA) and conventional energy absorption (CEA) approaches. Topologically, the design of the 3D metamaterials is founded on star-shaped unit cells herein. To achieve the PEA behavior, horizontal bars are merged into the parent star-shaped unit cell. This leads to introducing multistiffness unit cells (controllable unit-cell densifications) to provide stability and different peak force levels during compression. For further evaluation, finite element analysis (FEA) is employed. To illustrate the design functions during physical operation and validate the FEA, lattice-based metamaterials are fabricated from resin with a shape recovery property by an SLA 3D printer and tested mechanically. Close coincidence is observed between the FEA and the experiments, showing the accuracy of the modeling. A thermal test, via a heating–cooling process, is also carried out to display the shape recovery capability of metamaterials where plastic deformations are fully released, and samples get back to their original shapes. Finally, the newly proposed ZPRs are compared with conventional 3D reentrant metamaterials in terms of energy absorption capacity, demonstrating their considerable mechanical performances.

1. Introduction

Crashworthiness is the ability of the materials or structures to absorb impact energy through plastic deformations, friction, fracture, shear, bending, and even torsion.[1] Energy absorbers have been extensively used for different applications. The most prevalent applications can be found in the automotive, railway, and aerospace industries.[2,3] It is important to reduce the mortality rate caused by car crashes in the automotive industry. When it comes to passengers' safety, some critical crashworthy elements must be considered to design proper energy absorbers. The most vital item could be the initial reaction force caused by hitting an external object.[4] The lower the initial reaction force, the safer the occupants might be. A vehicle contains structural elements like rockers, pillars, and bumpers. Among these elements, the front bumper plays a vital role when it comes to energy absorption and is the most effective parameter for vehicle safety and occupants. The front bumper usually absorbs more than half of the kinetic energy during a car crash.[4] This is the main reason for magnifying the existence of high-performance energy absorbers

Distinct from the initial reaction force, the crashworthy designers have been considering various main criteria for an ideal energy absorber, including high energy absorption performance, stability, and safety. Consequently, some design approaches such as gradual energy absorption (GEA), piecemeal energy absorption (PEA), and conventional energy absorption (CEA) have been proposed.[5–7] The absorbers designed based on the PEA and GEA approaches show different peak force levels in force–displacement relation, whereas the CEA-based absorbers show a peak force level in their force–displacement relation. Xu et al.[5] proposed a structure exhibiting the GEA for subway vehicles. The proposed energy absorber exhibits multistiffness behavior under the impact, showing different peak force levels as well. Afterward, the concept of piecemeal energy absorption (PEA) was introduced by Esa et al.[6]. The PEA concept is similar to the GEA concept. Due to the flexibility of the PEA concept over the GEA, this concept is extended to diverse applications. The PEA strategy provides lower damages under low-velocity impact and higher energy absorption capacity under high-velocity impact. Apart from the GEA and PEA concepts, most energy absorbers possess a CEA response.[7] The CEA response means a gradual increase in initial reaction forces under the impact and then the fluctuations in crushing forces are caused by overcoming the energy absorber's yield strength.

R. Hamzehei, N. Wu
Department of Mechanical Engineering
University of Manitoba
Winnipeg, Manitoba R3T 5V6, Canada

A. Serjouei, M. Bodaghi
Department of Engineering
School of Science and Technology
Nottingham Trent University
Nottingham NG11 8NS, UK
E-mail: mahdi.bodaghi@ntu.ac.uk

A. Zolfagharian
School of Engineering
Deakin University
Geelong 3216, Australia

The ORCID identification number(s) for the author(s) of this article can be found under https://doi.org/10.1002/adem.202200656.

When it comes to energy absorbers, mechanical metamaterials could be a proper choice for impact applications.[8] Mechanical metamaterials are artificially designed and architected structures obtaining their mechanical performances from the unique design of their unit cells.[9] In other words, the mechanical performances of the metamaterials are independent of the parent material used for fabrication. Due to the versatile mechanical performance of the metamaterials, they are divided into several main groups, including positive Poisson's ratio (PPR) structures,[10] zero Poisson's ratio (ZPR) structures,[11–14] and negative indices mechanical metamaterials such as auxetics,[15–17] negative stiffness, and thermal expansion structures.[18–21]

From a designing point of view, 2D mechanical metamaterials are designed via repeating the unit cells along with the two principal in-plane directions, then extruding in third directions.[22] On the other hand, the 3D mechanical metamaterials are designed by repeating the unit cells along with the three principal directions.[23] In practice, due to the complexity of mechanical loadings, the 3D metamaterials could be more applicable than their 2D counterparts. It is also worth noting that the fabrication process could be challenging due to the complexity of the geometry of the 3D metamaterials. However, the advent of modern additive manufacturing (AM) technology has eased fabrication. Therefore, the design of 3D metamaterials has been getting increasingly comprehensive.

Shen et al. introduced a 3D auxetic metamaterial designed by adding small reentrant unit cells to the vertices of the parent unit cells.[24] Their design showed a higher Young's modulus and controllable elastic properties compared to the conventional 3D reentrant metamaterial. Wang et al.[25] proposed 3D octagonal honeycomb metamaterials with reentrant angles. Their study exhibited a unique hardening process with a gradual increase in structural stiffness under compression. Zhang et al.[26] proposed an antichiral-based metamaterial whose mechanical properties are dependent on geometrical parameters. Chen et al.[27] designed a 3D auxetic metamaterial in which the narrow ribs were embedded into the typical reentrant unit cells. Their design was not only better at shrinking under compression, but it also exhibited a significant enhancement of Young's modulus compared to its conventional counterpart.

From a structural standpoint, an architected structure could be designed with gradient items, so-called graded metamaterials. The most prevalent gradient items considered by the designers could be the diversity in unit cell designs, wall thicknesses, or even the materials used during fabrication.[28,29] The graded metamaterials could enhance mechanical properties such as energy absorption capacity, impact mitigation, and blast loadings.[30] Most research has focused on designing 2D graded metamaterials. In this regard, Hamzehei et al.[14] designed 2D bioinspired ZPR metamaterials for energy absorption applications with the simultaneous possession of stability. Li et al.[31] designed piecewise graded honeycombs to exhibit superior energy absorption capacity under high-velocity impact. Rahman et al.[32] considered different unit cell designs and the material used during fabrication to enhance energy absorption performance. Wu et al.[33] designed a bigraded honeycomb with diversity in wall thickness along with in-plane and out-plane directions. Their design showed high energy absorption capacity with low initial impact force. In contrast with 2D graded metamaterials, less research has been carried out on 3D graded metamaterials. Li

et al.[34] investigated the bending behavior of the 3D auxetic graded metamaterial with a diversity of wall thicknesses. Their study exhibited fewer lateral deflections compared to the nonauxetic one. They also designed a functionally graded (FG) 3D auxetic metamaterial to enhance structural buckling performance.
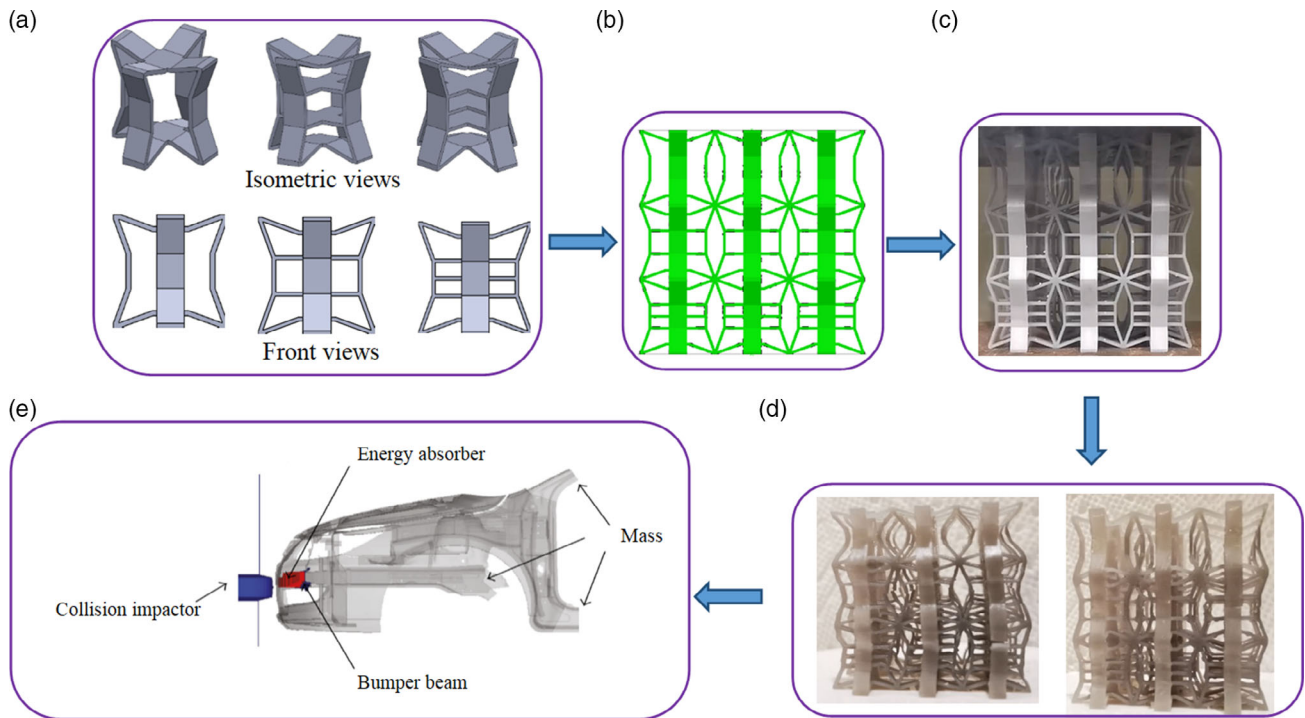
Mechanical metamaterials are also capable of exhibiting thermomechanical behaviors, so-called 4D printing concept, if their parent material is active (possessing shape memory effect).[35] Among active materials, shape memory polymers (SMPs) and hydrophilic polymers have been considered due to their capability of changing configurations.[36] 4D-printed structures can transform configurations in response to an external stimulus such as heating. In other words, 4D-printed structures can recover their initial shapes when heated over the glass transition temperature. Due to the functionality of the 4D printing concept, the 4D-printed metamaterials are extensively used for various applications. For biomedical applications,[37] the 4D printing concept is considered to fabricate biological structures such as implants, scaffolds, and stents. The 4D printing concept is also practical where energy absorption applications are necessitated. In this regard, Bodaghi et al.[38] introduced planar single and dual-material metamaterials via FDM 4D printing technology. Their study showed fully reversible deformation behaviors, and the simultaneous possession of dissipating energy and hysteresis curves. In another work,[39] they compared reversible energy absorption applications of auxetic, hexagonal, and AuxHex structures, shedding light on the capability of auxetic structures when it comes to energy absorption applications. In addition, they have looked into how 4D-printed sandwich structures could be used for energy absorption applications.[40]

The literature review discloses the importance of 3D energy absorbers to exhibit low initial reaction forces, stability, and high energy absorption capacity under quasistatic compression. The current study introduces novel 3D ZPR metamaterials for reversible energy absorption applications additively manufactured by 4D printing technology. To design 3D meta-energy absorbers, two energy-absorbing criteria, namely, PEA and CEA, are taken into account. Multistiffness unit cells are designed in a way that local densification can be controlled under compression. This yields different peak force levels in a force–displacement relationship, resulting in a higher energy absorption capacity. The 4D-printed metamaterials possess a full shape recovery behavior after a heating–cooling process. A finite element analysis (FEA) is also developed to accurately replicate the mechanical responses of the 3D metamaterials. The proposed meta-absorbers are finally compared with conventional 3D auxetic metamaterials in terms of energy absorption capacity and stability, approving the considerable superiority of the proposed energy absorbers. The introduced designs would be expected to pave the way for the designers to consider diverse unit cell arrangements with variable stiffness adapted for a specific compressive response.

2. Conceptual Design

2.1. Overview of the Work

Figure 1 shows a flowchart of the design process in this study. This begins with designing three fundamental unit cells

ADVANCED
SCIENCE NEWS
www.advancedsciencenews.com

ADVANCED
ENGINEERING
MATERIALS
www.aem-journal.com

Figure 1. a) Unit cell design, b) FEA, c) experiments, d) shape recovery feature, and e) car bumper as a possible application.[41]

(Figure 1a). Then, the study follows up on the investigation of deformation patterns of the metamaterials via the FEA and experiments (Figure 1b,c). The shape recovery behavior of the meta-absorbers is also investigated (Figure 1d). A future possible application of the proposed meta-absorbers could be in car bumpers (Figure 1e). This work is dedicated to developing a new generation of 3D metamaterials with a high energy absorption capability and a shape recovery feature.

2.2. Metamaterials Design Criterion

The criterion for designing metamaterials is based on the peak force levels under quasistatic compression. **Figure 2** shows the models considered for this purpose, so-called model—A, B, C, D, E, F, and G. More information on the structural design process can be found in the Supporting Information.

2.3. Fabrication, Mechanical Testing, and FEA

The 3D meta-absorbers are fabricated by an SLA 3D printer. A quasistatic compression test is carried out on the 3D metamaterials. An FEA is also performed to simulate the deformation patterns of metamaterials. Finally, a heating–cooling process is performed after unloading the experimental samples to investigate the shape recovery feature of the energy absorbers. More details in regard to the fabrication process, mechanical tests, and the FEA procedure are provided in the Supporting Information.

3. Results and Discussions

Firstly, the most common energy-absorbing indicators are defined. Energy absorption (EA) is defined as the integration of crushing force concerning displacement, x. Thus, the absorbed energy of stage-i (EA$_i$) (Equation (1)) and the total absorbed energy (Equation (2)) can be formulated as follows. In these equations, the letters "i" and "n" indicate the first and an arbitrary stage of the force–displacement relationship.

$$EA_i = \int_{x_i}^{x_n} F(x)\, dx \tag{1}$$

$$EA = \sum_{i}^{n} EA_i \tag{2}$$

Specific energy absorption (SEA) is defined as the absorbed energy by a structure per unit of mass (Equation (3)).

$$SEA = EA/M \tag{3}$$

Stroke length indicates the distance that an absorber can deform until entering the full densification zone of the force–displacement relationship.[42] From a structural point of view, a desirable energy absorber is the one exhibiting a long stroke length, and possessing low initial reaction force as well (discussed in detail in the next sections).
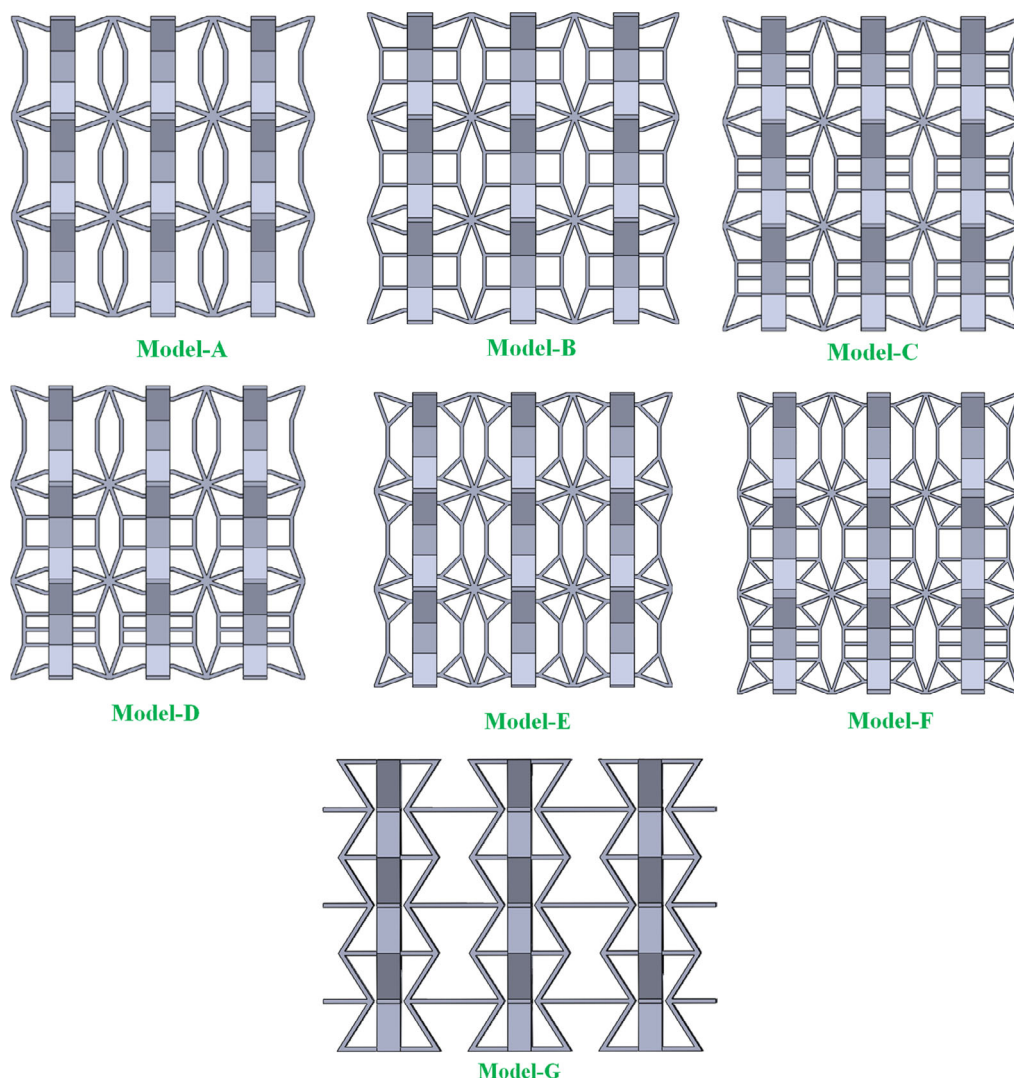
Figure 2. Various 3D meta-absorbers.

3.1. Deformation Modes

This section investigates the reason why an octagonal unit cell is merged into the initial star-shaped unit cell (the difference between models A and E is investigated). Then, the energy absorbers are classified according to the PEA (different peak levels) and CEA (one peak level) methodologies, and the deformation patterns will be explained in detail.

3.1.1. Difference between Models "A" and "E"

Figure 3 illustrates the deformation patterns of model "A" under quasistatic compression. Bending is the most dominating mode of deformation. The parent model "A" shows CEA behavior with one peak force level (see Figure S6a, Supporting Information). This means that the model "A" demonstrates a positive stiffness behavior upon applying compressive displacements, until overcoming the initial resistance of the structure at 4 mm, and then exhibits some fluctuations in force–displacement response.

To boost the energy absorption capacity of model "A", an octagonal unit cell is merged into the parent star-shaped unit cell (see Figure S1, Supporting Information). When merged, the octagonal unit cell leads to the creation of triangles at the corners of the parent star-shaped unit cell. This gives rise to a gradual increase in structural stiffness, and a higher energy absorption capacity compared to the parent model "A". **Figure 4**a shows the deformation patterns of model "E" under quasistatic compression. Once a compressive displacement is applied, the triangles commence rotating. In essence, the triangles not only lead to facilitating the bending of the walls, due to the rotation, but also increase structural stiffness and energy absorption capacity compared to the parent structure (model "A") (see Figure 4b). Considering the model "E", an SEA increase by up to 92% (from 1.06366 to 2.04969) is found in the SEA compared to the model "A" (see Figure 4c). It is also worth noting that the model "E" possesses CEA behavior, though different peak force levels can be seen in the force–displacement response (as shown in Figure 4b). In other words, only when the model "E" deforms
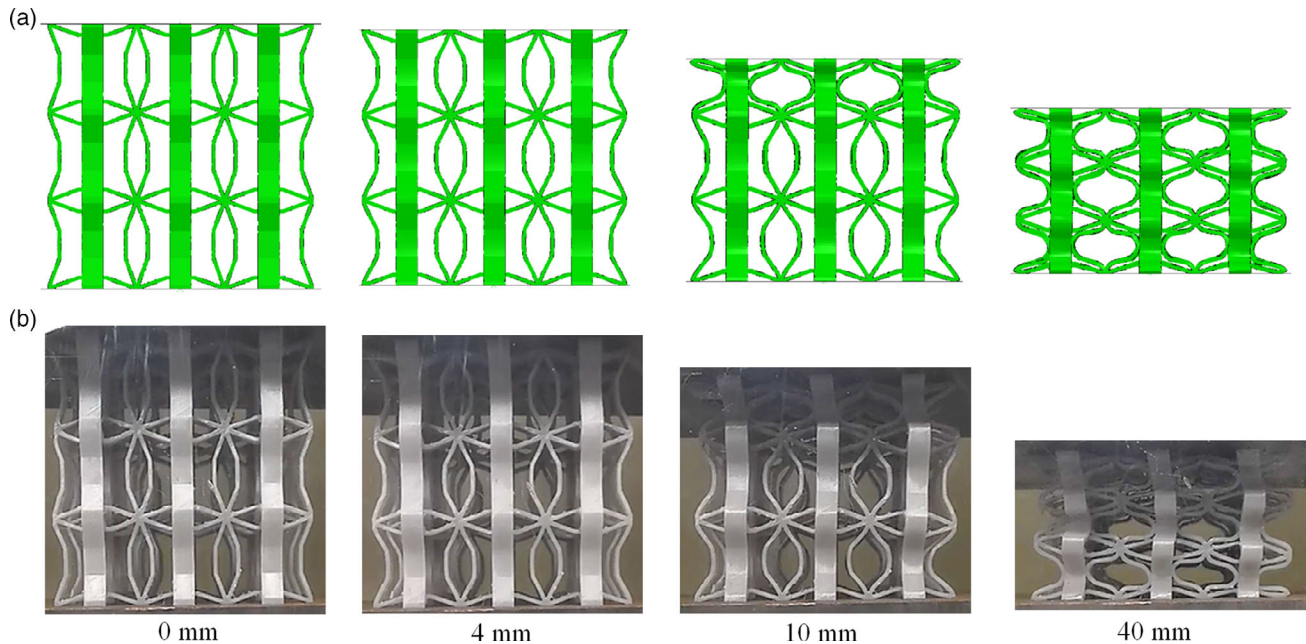
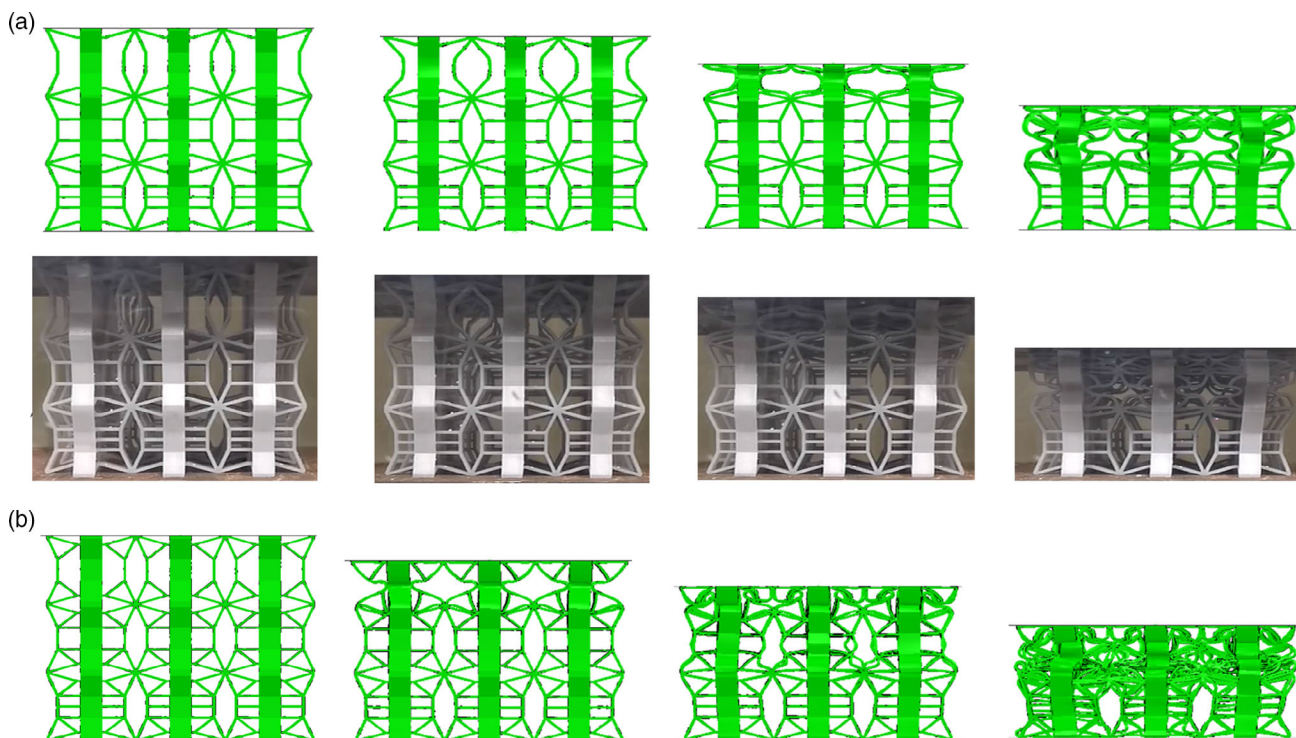**Figure 3.** The deformation patterns of model "A" obtained from the a) FEA and b) experiment.
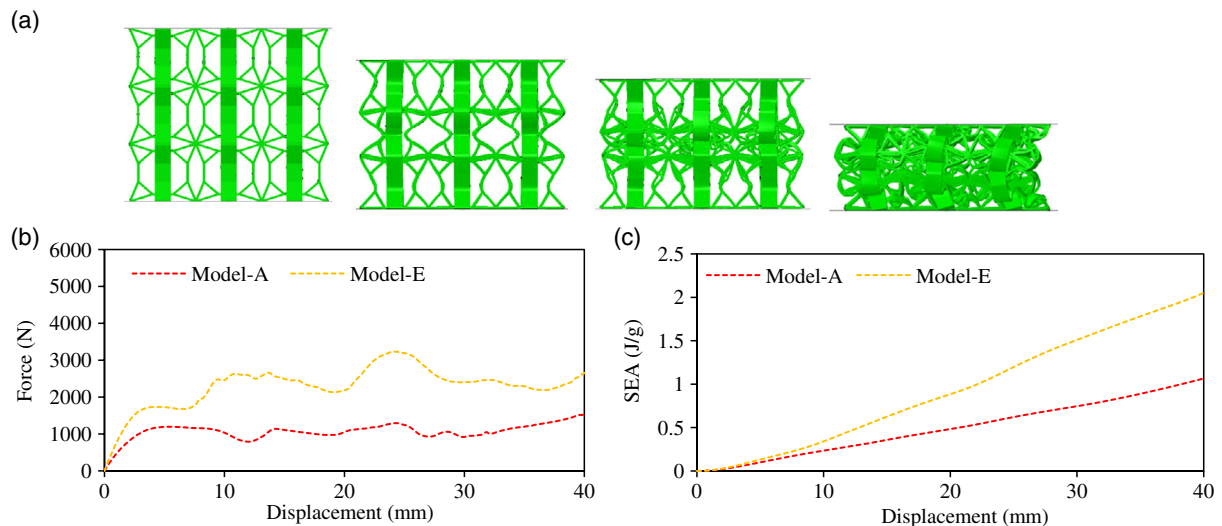
Figure 4. a) Meta-absorber "E" deformation patterns, b) force–displacement, and c) SEA–displacement curves of meta-absorbers "A" and "E".

orderly, i.e., stage by stage, it could exhibit PEA behavior. That is due to the fact that each stage of deformation patterns exhibits an exclusive peak force level higher than that of the previous stages during compression.

3.1.2. The PEA-Based Energy Absorbers

When it comes to energy absorber design, the PEA criterion means an absorber exhibiting a stage-by-stage deformation pattern during compression. These deformation patterns are caused by gradual structural stiffness. Thus, the PEA approach

can be seen in an absorber with sequential weak-to-strong deformation modes. In this case, each stage has a unique energy absorption characteristic. It is equivalent to the fact that the PEA-based energy absorbers can also control the reaction forces during crush. This type of energy absorber can also possess a long stroke length. Consequently, the PEA-based energy absorbers could be reasonable to absorb kinetic energy in a car crash to provide occupants' safety. Here, the models "D" and "F" have been designed based on the PEA methodology. As shown in **Figure 5**, the deformation patterns occur stage by stage due to the gradual differences in structural stiffness. What provides a considerable difference in the structural

**ADVANCED
SCIENCE NEWS**

www.advancedsciencenews.com

**ADVANCED
ENGINEERING
MATERIALS**

www.aem-journal.com

**Figure 5.** The deformation patterns of meta-absorbers a) "D" and b) "F" under compression.

stiffness is the existence of horizontal bars in the second and third layers of the meta-absorbers. The more horizontal bars, the higher is the stiffness. This also leads to providing stability for the structure during compression, avoiding the occurrence of the transverse deformations in the structures with the same stiffness (see Figure 3b and 4a). In other words, the metamaterials comprising the unit cells with the same stiffness are probable to show instabilities under compression. This phenomenon could be more obvious in the experiments due to the defects that occur during fabrication.

The force–displacement and SEA–displacement relationships of these models can be seen in **Figure 6**a,b. It can be inferred from Figure 6a that each peak force level corresponds to the failure of each layer of meta-absorbers "D" and "F". The reaction forces increase step-by-step under compression, which is in parallel with the PEA concept.

3.1.3. The CEA-Based Energy Absorbers

Like most common energy absorbers, the models "A", "B", "C", and "E" exhibit conventional mechanical performance. This means that a gradual increase in reaction forces at low displacements and then some fluctuations in the force–displacement relationship can be seen (see **Figure 7**). Take models "A" and "B" as examples. These absorbers can be used in applications, where high structural stiffness is required at low compressive displacements, like shock impact applications. Figure 7b exhibits the SEA–displacement relation of the absorbers.

Figure 8 demonstrates the superiority of the newly designed 3D ZPR energy absorbers in terms of the SEA, in particular PEA-based energy absorbers (models "D" and "F"), compared to the conventional 3D auxetic metamaterial (model G). It is found that the energy absorption capacity of model "F" is almost 4 times
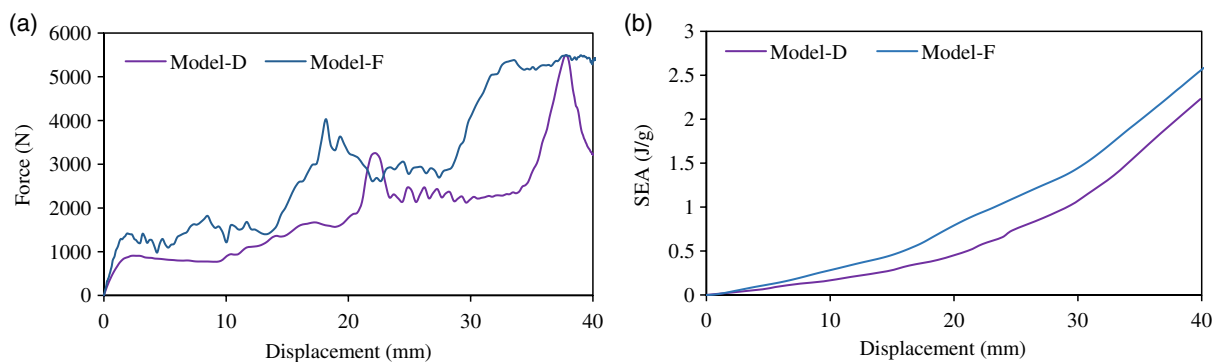
Figure 6. The a) force–displacement and b) SEA–displacement relations of models "D" and "F" under compression obtained from FEA.
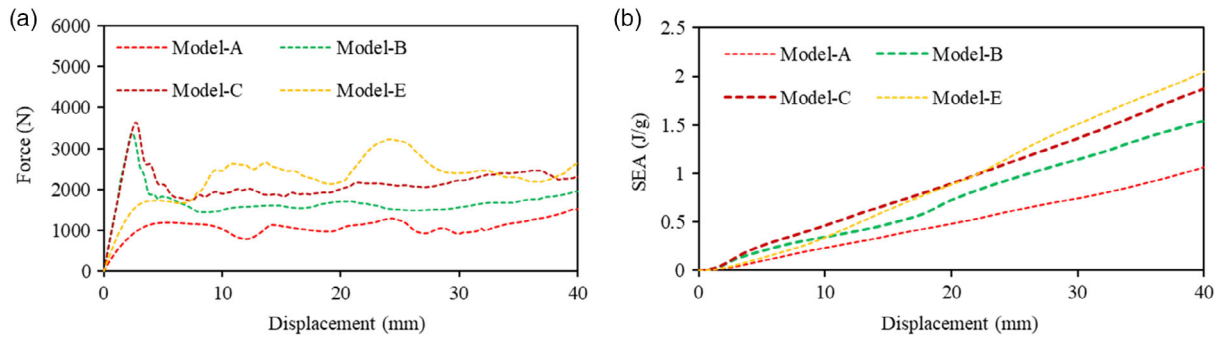
Figure 7. The a) force–displacement and b) SEA–displacement relations of models "A", "B", "C", and "E" obtained from FEA.
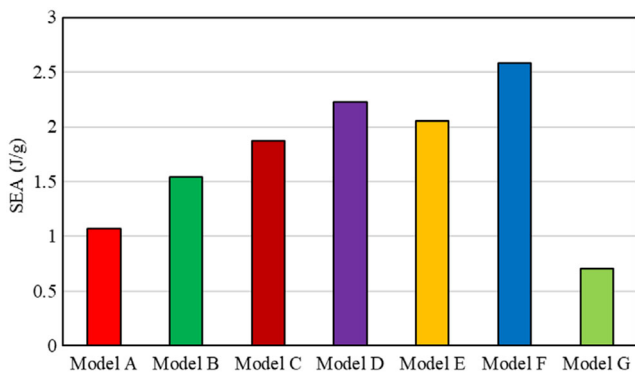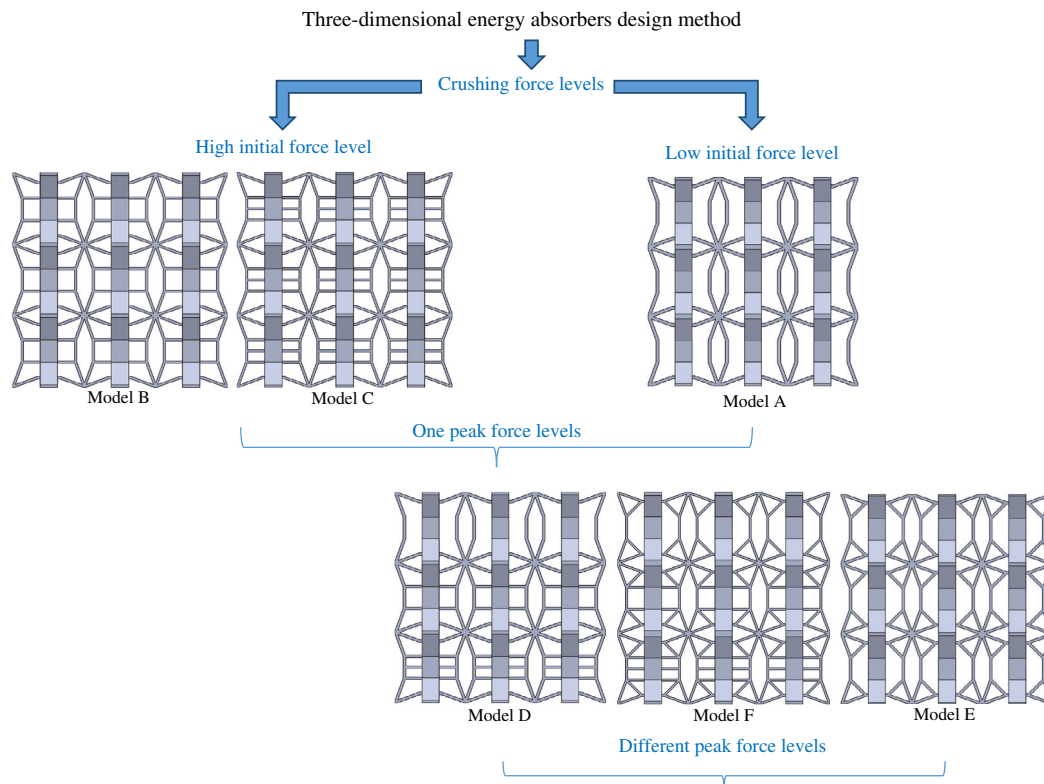

Figure 8. A comparison between newly designed 3D ZPRs and conventional auxetic metamaterial (model G).
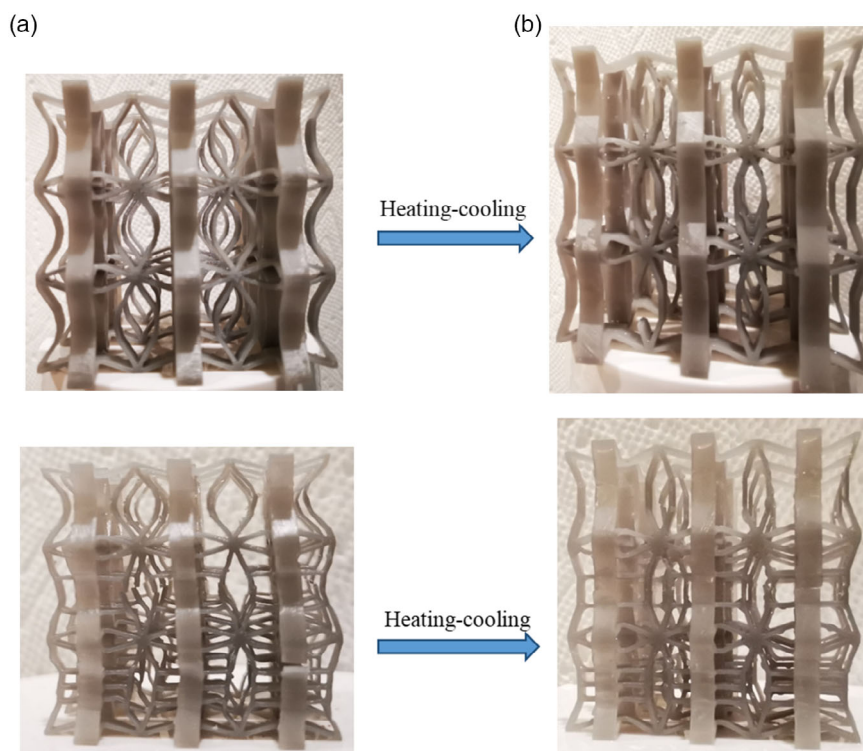
greater than that of the conventional reentrant metamaterial (model "G"). It confirms the high mechanical performance of the proposed meta-absorbers.

3.1.4. Classification of Energy Absorbers

As discussed earlier, the energy absorbers possess different mechanical behaviors when compressed. This includes those with high and low initial reaction forces at low compressive displacements. Apart from the initial reaction forces, diverse peak force levels can be seen in force–displacement relationships. **Figure 9** provides a classification of energy absorbers based on their mechanical performances introduced in this article.

Figure 9. Classification of energy absorbers.

**ADVANCED
SCIENCE NEWS**

www.advancedsciencenews.com

**ADVANCED
ENGINEERING
MATERIALS**

www.aem-journal.com

Figure 10. a) Before and b) after heating–cooling procedure on samples for demonstrating shape recovery.

3.1.5. Shape Recovery Feature

This section investigates the effect of heating the samples, then cooling them down to room temperature, to recover the samples' original shapes. **Figure 10** shows the configuration of samples after the unloading and heating–cooling processes. After unloading, the structures tend to elastically recover their original shapes. Although the residual plastic strains and fractures exist at large strain rate, the structures recover fully (see Figure 10a). Figure 10b reveals that by heating the metastructures, the plastic strains are released and the samples fully recover their original shapes except the fracture parts. It confirms that the shape memory metastructures have a full recovery feature.

3.1.6. Reusability after Shape Recovery

This section describes the mechanical performances of the 4D metamaterials after shape recovery. The force–displacement relations of metamaterials with their original and 50% scaled-down dimensions after the second compression are presented in **Figure 11**.

For the 4D metamaterials with their original dimensions, the structure "A" shows similar force–displacement relations after two cyclic loadings (see Figure 11a). However, the structure "D" exhibits different peak force levels during compression after the first and second cyclic loadings. For the structure "D", the discrepancies between the force–displacement relations of the
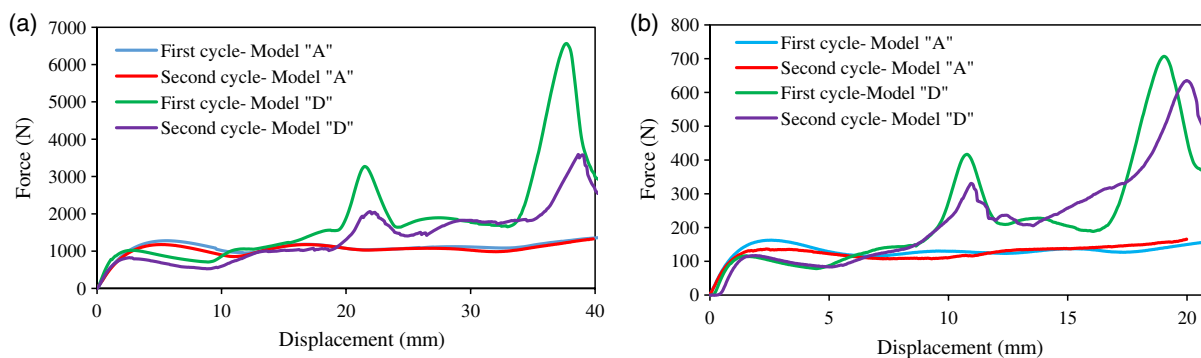
Figure 11. First and second cyclic loadings on a) original and b) 50% scaled-down samples.
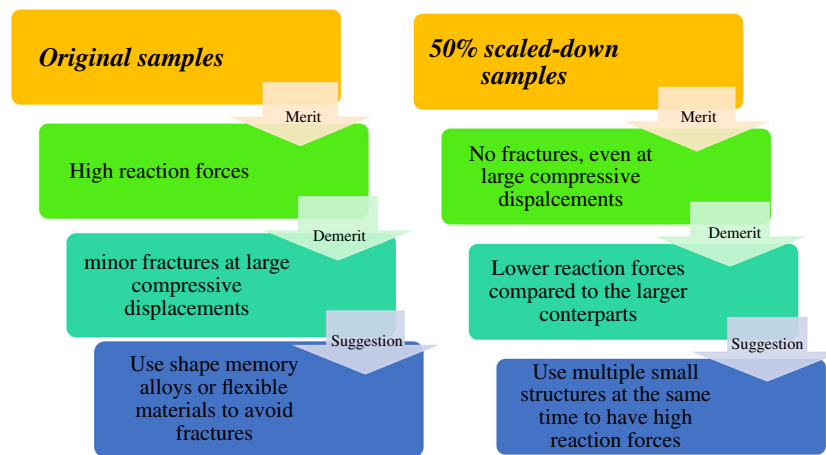
Figure 12. First and second cyclic loadings on a) original and b) 50% scaled-down samples.

first and second cyclic loading are related to the fractures caused by bending of the walls in some parts of the metamaterial at high compressive displacements. Due to the fact that the smaller the wall thickness, the more facilitation the walls possess to bend, the original samples were scaled down by 50%. Figure 11b shows a close coincidence between the first and second cyclic loadings. It is worth mentioning that although fewer and minor fractures were seen in the scaled-down structures compared to the fractures that occurred in the samples with original dimensions after two cyclic loadings, the reaction forces of 50% scaled-down samples are smaller than the reaction forces of their counterparts with original dimensions (cf., Figure 11a,b). The possibility to avoid fractures under quasistatic compression could be the use of either shape memory alloys (SMAs) or flexible materials for fabrication. A summary of the size effects on the mechanical performances of the 4D metamaterials is provided in **Figure 12**.

4. Concluding Remarks

This study introduced high-performance 3D metamaterials for reversible energy absorption applications fabricated by an SLA 3D printer. The designs were drawn based on piecemeal and conventional energy absorption criteria (PEA and CEA, respectively). Resin-based metamaterials were fabricated by 4D printing technology, and tested mechanically to verify the FEA and thermally to check their reversibility. The conclusions are summarized as follows. 1) The parent metamaterial contains star-shaped unit cells, showing CEA behavior with one peak force level on a force–displacement relationship. 2) A PEA-based energy absorber requires multistiffness unit cells in its construction to exhibit different peak force levels. To achieve this, horizontal bars are merged into the initial star-shaped unit cell, leading to a metamaterial with variable stiffness. 3) The model "F", designed based on the PEA criterion, has the highest energy absorption capacity. 4) The energy absorption capacity of the newly designed metamaterial (model "F") enlarges up to 267% compared to a conventional 3D reentrant metamaterial. 5) Fully shaped recovery, so-called 4D, behaviors are seen after heating and cooling the samples. 6) The independency of 4D metamaterials'

mechanical performances on the scale sizes. 7) Apart from energy absorption applications, the proposed metamaterials can be used for biomedical applications for possible future studies, for example, as soft tactile sensors, where multiple sensitivities are required.

Supporting Information

Supporting Information is available from the Wiley Online Library or from the author.

Conflict of Interest

The authors declare no conflict of interest.

Data Availability Statement

The data that support the findings of this study are available in the supplementary material of this article.

[1] R. A. Eshkoor, S. A. Oshkovr, A. B. Sulong, R. Zulkifli, A. K. Ariffin, C. H. Azhari, *Mater. Des.* **2013**, *47*, 248.
[2] H. Mansoori, R. Hamzehei, S. Dariushi, *Proc. Inst. Mech. Eng. Part L* **2022**, *236*, 647.

[3] R. Bejjani, S. Odelros, S. Öhman, M. Collin, *Proc. Inst. Mech. Eng. Part L* **2021**, *235*, 114.

[4] *Nonlinear Approaches In Engineering Applications: Advanced Analysis Of Vehicle Related Technologies* (Eds: Reza N., Jazar, Liming Dai), Springer, Berlin **2016**.

[5] P. Xu, C. Yang, Y. Peng, S. Yao, D. Zhang, B. Li, *Int. J. Mech. Sci.* **2016**, *107*, 1.

[6] M. Esa, P. Xue, M. Zahran, M. Abdelwahab, M. Khalil, *Thin-Walled Struct.* **2017**, *111*, 176.

[7] M. S. Zahran, Pu. Xue, M. S. Esa, M. M. Abdelwahab, *Thin-Walled Struct.* **2018**, *122*, 64.

[8] R. Hamzehei, S. Rezaei, J. Kadkhodapour, A. P. Anaraki, A. Mahmoudi, *Mech. Mater.* **2020**, *142*, 103291.

[9] S. Rezaei, J. Kadkhodapour, R. Hamzehei, B. Taherkhani, A. P. Anaraki, S. Dariushi, *Photonics and Nanostruct. Fundam. Appl.* **2021**, *43*, 100868.

[10] N. S. Ha, T. M. Pham, T. T. Tran, H. Hao, G. Lu, *Composites Part B: Eng.* **2022**, *236*, 109818.

[11] Y. Chen, B.-B. Zheng, M.-H. Fu, L.-H. Lan, W.-Z. Zhang, *Smart Mater. Struct.* **2018**, *27*, 045003.

[12] A. Zolfagharian, M. Bodaghi, R. Hamzehei, L. Parr, M. Fard, B. F. Rolfe, *Sustainability* **2022**, *14*, 6831.

[13] J. Huang, X. Gong, Q. Zhang, F. Scarpa, Y. Liu, J. Leng, *Composites Part B: Eng.* **2016**, *89*, 67.

[14] R. Hamzehei, A. Zolfagharian, S. Dariushi, M. Bodaghi, *Smart Mater. Struct.* **2022**, *31*, 035001.

[15] D. Li, J. Yin, L. Dong, R. S. Lakes, *J. Mater. Sci.* **2018**, *53*, 3493.

[16] W. Lv, D. Li, L. Dong, *Int. J. Mech. Sci.* **2021**, *191*, 106105.

[17] D. Li, G. Shen, *Smart Mater. Struct.* **2022**, *31*, 065017.

[18] C. Morris, L. Bekker, C. Spadaccini, M. Haberman, C. Seepersad, *Adv. Eng. Mater.* **2019**, *21*, 1900163.

[19] Z. Wang, C. Luan, G. Liao, J. Liu, X. Yao, J. Fu, *Adv. Eng. Mater.* **2020**, *22*, 2000312.

[20] J. K. Wilt, C. Yang, G. X. Gu, *Adv. Eng. Mater.* **2020**, *22*, 1901266.

[21] R. Hamzehei, J. Kadkhodapour, A. P. Anaraki, S. Rezaei, S. Dariushi, A. M. Rezadoust, *Int. J. Mech. Sci.* **2018**, *145*, 96.

[22] W. Zhang, S. Zhao, F. Scarpa, J. Wang, R. Sun, *Thin-Walled Struct.* **2021**, *159*, 107191.

[23] R. Valle, G. Pincheira, V. Tuninetti, *Proc. Inst. Mech. Eng., Part L* **2021**, *235*, 1341.

[24] L. Shen, X. Wang, Z. Li, K. Wei, Z. Wang, *Mater. Des.* **2022**, *216*, 110527.

[25] S. Wang, C. Deng, O. Ojo, B. Akinrinlola, J. Kozub, N. Wu, *Composite Struct.* **2022**, *280*, 114882.

[26] H. Zhang, J. Cui, G. Hu, B. Zhang, *Int. J. Smart Nano Mater.* **2022**, *13*, 1.

[27] Y. Chen, M.-H. Fu, *Smart Mater. Struct.* **2017**, *26*, 105029.

[28] M. Alshaqaq, A. Erturk, *Smart Mater. Struct.* **2021**, *30*, 015029.

[29] F. Xu, X. Zhang, H. Zhang, *Eng. Struct.* **2018**, *171*, 309.

[30] N. Novak, M. Borovinšek, M. Vesenjak, M. Wormser, C. Körner, S. Tanaka, K. Hokamoto, Z. Ren, *Phys. Status Solidi B* **2019**, *256*, 1800040.

[31] Z. Li, Y. Jiang, T. Wang, L. Wang, W. Zhuang, D. Liu, *Composite Struct.* **2019**, *207*, 425.

[32] H. Rahman, E. Yarali, A. Zolfagharian, A. Serjouei, M. Bodaghi, *Materials* **2021**, *14*, 1366.

[33] Y. Wu, L. Sun, P. Yang, J. Fang, W. Li, *Thin-Walled Struct.* **2021**, *164*, 107810.

[34] C. Li, H.-S. Shen, H. Wang, *Nonlinear Dyn.* **2020**, *100*, 3235.

[35] S. Choi, B. Park, S. Jo, J. H. Seo, W. Lee, D.-G. Kim, K. B. Lee, Y. S. Kim, S. Park, *Adv. Eng. Mater. 24*, 2101497.

[36] T. Liu, T. Zhou, Y. Yao, F. Zhang, L. Liu, Y. Liu, J. Leng, *Composites Part A: Appl. Sci. Manuf.* **2017**, *100*, 20.

[37] S. Shakibania, L. Ghazanfari, M. Raeeszadeh-Sarmazdeh, M. Khakbiz, *Drug Dev. Ind. Pharm.* **2021**, *47*, 521.

[38] M. Bodaghi, A. Serjouei, A. Zolfagharian, M. Fotouhi, H. Rahman, D. Durand, *Int. J. Mech. Sci.* **2020**, *173*, 105451.

[39] N. Namvar, A. Zolfagharian, F. Vakili-Tahami, M. Bodaghi, *Smart Mater. Struct.* **2022**, *31*, 055021.

[40] A. Serjouei, A. Yousefi, A. Jenaki, M. Bodaghi, M. Mehrpouya, *Smart Mater. Struct.* **2022**, *31*, 055014.

[41] F. Mo, S. Zhao, C. Yu, Z. Xiao, S. Duan, *Appl. Bionics Biomech.* **2018**, *2018*, 1.

[42] M. S. Zahran, P. Xue, M. S. Esa, M. M. Abdelwahab, G. Lu, *Lat. Am. J. Solids Struct.* **2017**, *14*, 292.